Desalination and Water Treatment
www.deswater.com

doi: 10.1080/19443994.2015.1074115

57 (2016) 15455–15466
July

Taylor & Francis
Taylor & Francis Group

Selective adsorption of Zn^{2+} on surface ion-imprinted polymer

Tieming Yu[a,b], Xvsheng Qiao[a,*], Xuhui Lu[c], Xianping Fan[a]

[a]*State Key Laboratory of Silicon Materials, School of Materials Science and Engineering, Zhejiang University, Hangzhou 310027, P.R. China, Tel. +86 572 6822137; email: timyutm@163.com (T. Yu), Tel. +86 571 87951234; emails: qiaoxus@zju.edu.cn (X. Qiao), fanxp@zju.edu.cn (X. Fan)*
[b]*Zhejiang Chang'an Renheng Technology Co., Ltd, Changxing 313113, P.R. China*
[c]*Department of Materials Science and Engineering, Missouri University of Science & Technology, 223 McNutt Hall, 1400 N. Bishop, Rolla, MO 65409-0340, USA, Tel. +1 6014666485; email: xuhui.lu@gmail.com*

Received 28 May 2014; Accepted 8 July 2015

ABSTRACT

A new type of Zn^{2+} ion-imprinted polymer (Zn^{2+}-IIP) was synthesized on the surface of attapulgite, displaying high affinity and selectivity to Zn^{2+}. Fourier transform infrared spectra (FTIR) revealed Zn^{2+}-IIP to be an organic–inorganic hybrid polymer, with Zn^{2+} imprinted cavities formed by CTS groups and connected to the surface of the attapulgite by A-187 cross-linked network. The adsorption kinetic investigation showed that the adsorption of Zn^{2+}on Zn^{2+}-IIP was a pseudo-second-order process. The maximum adsorption capacities of Zn^{2+} were 0.536, 0.665, 0.715, and 0.722 meq/g at 288, 298, 308, and 318 K, respectively, where the activation energy, E_a, was evaluated as 23.8 kJ/mol. By thermodynamic study, ΔH° and ΔS° of the adsorption were determined as 30.862 kJ/mol and 108.664 J/mol K, respectively, while the negative ΔG° decreased with rising temperatures, indicating that the adsorption process was feasible and spontaneous. The adsorption selectivity of the Zn^{2+}-IIP was also investigated via competitive adsorption of Zn^{2+}, Cd^{2+}, Cs^{+}, Co^{2+}, Ba^{2+}, Sr^{2+}, and Pb^{2+} from a mixture, demonstrating that Zn^{2+}-IIP had the capability of recognizing Zn^{2+} with high affinity and selectivity. The study of multi adsorption–desorption cycles showed that the Zn^{2+}-IIP can be reused many times without a significant decrease in the adsorption capacity.

Keywords: Adsorption; Zn^{2+}; Ion-imprinted polymer

1. Introduction

Contamination of waters by heavy metal ions from the discharge of industrial wastewater causes a worldwide environmental problem. Cadmium (Cd), lead (Pb), copper (Cu), and zinc (Zn) ions are among the most common heavy metal ions found in industrial effluents [1,2]. Zn^{2+} is often found in effluents discharged from industries, such as galvanizing plants, acid mine drainage, natural ores, and municipal wastewater treatment plants [3,4]. Zn^{2+} is not biodegradable and travels through the food chain via bioaccumulation. According to the World Health Organization, the maximum acceptable concentration of zinc in drinking water is 5 mg/L [5]. And, its toxicity for humans is 100–500 mg/d [6]. Therefore, removing excess of zinc from wastewater is of great importance. Numerous methods are currently

*Corresponding author.

employed, including carbon adsorption, ion exchange, chemical oxidation and reduction, membrane separation, electrolytic treatment, liquid extraction, coagulation, evaporation, electro precipitation, flotation, hydroxide and sulfide precipitation, ultra filtration, crystallization, and electrodialysis [7–9]. Adsorption is one effective method for removing zinc [10,11].

Ion-imprinted polymers (IIPs) prepared by molecular imprinting technique are some of the developed adsorbents for the selective removal of heavy metals [12]. An ion-imprinted polymer is synthesized by co-polymerizing template ions with suitable monomers. Then, template ions are removed and imprinted cavities are created. The cavities provide tailor-made binding sites for the template ions removed from the ion-imprinted polymer [13,14]. So, IIPs are effective and selective adsorbents for their respective imprinting ions [13,15,16].

However, most of the traditional IIPs exhibit high selectivity but poor site accessibility to the target ions because many of the functional groups and template ions are embedded inside the polymer network, and mass transfer is difficult [17]. Surface imprinting is a feasible solution to this problem. Surface ion imprinting technique is one of the important synthesizing methods of IIP and has outstanding advantages, e.g. simple and convenient preparation, and high selectivity [18]. Currently, several studies have reported ion-imprinted polymer based on surface imprinting with selective adsorptions of heavy metal ions, such as cadmium and copper ions, but few is about zinc ions [19]. Thus, it is of great value to prepare a new adsorbent using surface imprinting method in order to ion selectively remove Zn^{2+} from wastewater. In this study, a novel ion-imprinted polymer was synthesized on the surface of attapulgite. The Zn^{2+} adsorption behavior of the IIP was also studied. Meanwhile, a complex system containing Zn^{2+} (e.g. effluents and wastewater) also contain many other metal ions [20–22], such as Cs^{+}, Sr^{2+}, Ba^{2+}, Cu^{2+}, Co^{2+}, Ni^{2+}, Pb^{2+}, Cd^{2+}, Mn^{2+}, Cr^{3+}, V^{5+}, and As^{5+}. Therefore, this study also investigated the selective adsorption of Zn^{2+} onto IIP among a range of trace elements: Cd^{2+}, Cs^{+}, Co^{2+}, Ba^{2+}, Sr^{2+}, and Pb^{2+}.

2. Materials and methods

2.1. Materials

Chitosan (CTS), zinc sulfate heptahydrate ($ZnSO_4{\cdot}7H_2O$) (both from Sinopharm Chemical Reagent Co., Ltd, Beijing, China) and cross-linking agent Ethenyltrimethoxysilan (A-187) (from Union Carbide Corporation, USA) were used in the present work. The attapulgite was supplied by Sino Material (Xuyi, China). Doubly deionised water (DDW) was used throughout this work.

2.2. Synthesis of Zn^{2+} ion-imprinted polymer

Stock solution of metal was prepared using zinc sulfate heptahydrate ($ZnSO_4{\cdot}7H_2O$) in distilled water. 10 mL of $ZnSO_4$ solution (1 mol/L) and 5 g of CTS were added to 100 mL of 0.1 mol/L acetic acid aqueous solution at 35°C. Then, 10 g of attapulgite powder was added into the solution. After stirring for 1 h, 15 mL of A-187 was added into the solution to form a mixture. The mixture was stirred for 4 h to synthesize the polymer. After that, the moist mixture was kept at room temperature and ambient pressure for 24 h, allowing for evaporation, to complete the polymerization. The dried polymer product was ground to a fine powder and was washed with DDW to remove non-bound Zn^{2+}. The polymer was consequently treated with 1.0 mol/L HNO_3 for 24 h at room temperature to completely leach out the coordinated Zn^{2+}. The polymer was rinsed several times with DDW and was neutralized with 1.0 mol/L NaOH. The resulting adsorbent containing Zn^{2+} cavities was washed, filtered with DDW, and dried. The product was ground to a fine powder and sized with 80-mesh sieve and stored for further use. By comparison, the non-ion-imprinted polymer (NIP) was prepared as a blank in parallel without the addition of Zn^{2+}. The functional groups on ion-imprinted polymer were characterized by Fourier transform infrared spectroscopy (FTIR, Perkin-Elmer 580B) using KBr pellet. X-ray diffraction (XRD) measurements were performed on an XD-98 diffractometer with Cu Kα radiation ($\lambda = 0.154$ nm) at a scanning rate of 4°/min. The thermogravimetric analysis was carried out using a thermogravimetric analyzer at a heating rate of 10°C/min. The IIP samples were observed with a Hitachi S-4800 field emission scanning electron microscope.

2.3. Point of zero charge

The points of zero charge (PZC) of the samples were determined by the pH drift method [23]. A series of solutions of 0.01 mol/L NaCl had been boiled to remove dissolved CO_2 and then cooled to room temperature. Their pH values were adjusted to values between 1 and 10 using 0.1 mol/L HCl or 0.1 mol/L NaOH (recorded as initial pH). Then, the samples were immersed in each solution and the drift in the pH after 48 h (measured as final pH) was recorded. Since the sample in a solution (with a particular pH)

induces a drift in the pH toward the PZC, the pH value that did not drift after the addition of the sample was taken as the PZC. All measurements were carried out in triplicates.

2.4. Adsorption experiments

The ion-imprinted polymer was dispersed in 500 mL Zn^{2+} solution at a pH value of 6.0. The weight of ion-imprinted polymer was 0.5 g, except when the amount of ion-imprinted polymer was considered. The concentration of the Zn^{2+} solution was 0.77 meq/L, except when the concentration of the Zn^{2+} was considered. For kinetic studies, samples were withdrawn at specific intervals at 25 ± 1°C. For the isotherm studies, 50 mL suspension was shaken at 25°C for 360 min with initial Zn^{2+} concentration ranging from 0.077 to 1.23 meq/L. The procedure was repeated at 15, 35, and 45°C for thermodynamic studies. The dispersion was conducted on a horizontal shaker. The separation of IIP from the extracted metal solution was performed with a centrifuge (Sigma) at 5,000 rpm for 5 min. The residual Zn^{2+} concentration in the supernatant was analyzed with atomic absorption spectroscopy.

To determine Zn^{2+} uptake quality by the adsorbent, the equilibrium amount of the zinc adsorbed by adsorbent, Q_e (meq/g), was calculated using:

$$Q_e = \frac{(C_0 - C_e)V}{m} \quad (1)$$

where C_0 and C_e are the initial and equilibrium concentrations of Zn^{2+} ions in solution (meq/L), respectively, V is the volume of the aqueous phase (L), and m is the dry weight of the adsorbent (g).

The distribution coefficient (K_d), selectivity coefficient (K), and relative selectivity coefficient (K') were calculated according to the following equations:

$$K_d = \frac{(C_0 - C_e)V}{mC_e} \quad (2)$$

$$K = \frac{K_{d(Zn(II))}}{K_{d(M)}} \quad (3)$$

$$K' = \frac{K_{im}}{K_{non}} \quad (4)$$

where $K_{d(Zn(II))}$ is the distribution coefficient of the template metal ion Zn^{2+} and $K_{d(M)}$ is the distribution coefficient of the competing metal ions. K_{im} and K_{non} are the selectivity coefficients of the Zn^{2+} ion-imprinted polymer and the non-imprinted polymer, respectively. K' represents the difference in the metal adsorption affinity recognition of sites to the imprinted Zn^{2+} ions between them; the larger the K', the stronger the imprinted effect.

2.5. Desorption and reusability experiments

After the Zn^{2+} was adsorbed by the ion-imprinted polymer, the ion-imprinted polymer was treated with 50 mL of 1.0 mol/L HNO_3 at 50°C in a water bath for 12.0 h. The Zn^{2+} was leached from the adsorbent. Then, the concentration of Zn^{2+} in the solution was determined. Desorption ratio (R_d) was calculated from the following equation:

$$R_d = \frac{Q_d}{Q_e} \quad (5)$$

where Q_d is the amount of ions desorbed to the elution medium and Q_e is the amount of ions adsorbed onto the adsorbent. The ion-imprinted polymer was washed with DDW after each cycle of adsorption–desorption, then dried at 50°C and used in the next cycle.

3. Results and discussion

3.1. Characterization

The N–H stretching and O–H stretching vibrations can be characterized by the broad bands in the region of 3,200–3,500 cm^{-1} in Fig. 1(a), (b), (d), and (e), where CTS showed a much broader band at 3,460 cm^{-1} (Fig. 1(b)) than those of Zn^{2+}-IIPs at 3,420 cm^{-1}

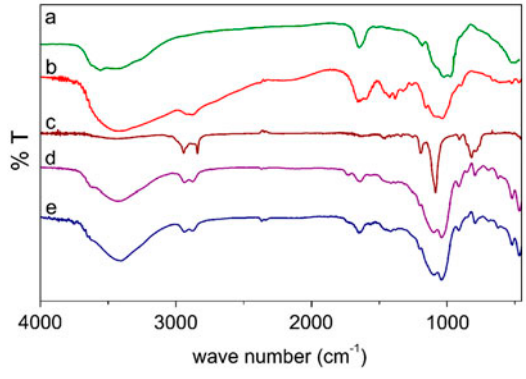

Fig. 1. FTIR spectra of the raw reagents to synthesize the Zn^{2+} ion-imprinted polymer (Zn^{2+}-IIPs): attapulgite (a), CTS (b), and A-187 (c) as well as FTIR spectra of the Zn^{2+} ion-imprinted polymer (Zn^{2+}-IIPs) before (d) and after (e) leaching coordinated Zn^{2+} ions.

(Fig. 1(d) and (e)). This indicated a reduced number of N–H and/or O–H, possibly due to the IIPs' synthesis reaction from attapulgite, CTS, and A-187. Compared with CTS (Fig. 1(b)), both the IIPs (Fig. 1(d) and (e)) had weakened N–H bending vibrations at 1,640 cm^{-1}, and had sharpened absorption bands of C–OH with shifts from 1,090 to 1,105 cm^{-1}. Those further suggested that a number of O–H and N–H in CTS were broken so that Zn^{2+} ions were coordinated with O and N to form Zn^{2+} templates surrounded by CTS array. By contrasting the Zn^{2+}-IIPs before (Fig. 1(d)) and after leaching (Fig. 1(e)), the latter had strengthened O–H and N–H stretching vibrations (at 3,420 cm^{-1}), maybe due to the breakages of Zn–N and Zn–O bonds and the subsequent recoordination of H–N and H–O bonds during the leaching process.

The double peaks at 2,840 cm^{-1} and 2,940 cm^{-1} in Fig. 1(b)–(e) could be assigned to the stretching vibrations of methyl ($–CH_3$) and methylene($–CH_2–$), and the small absorption bands around 1,465 cm^{-1} were also owing to the methyl and/or methylene deformation vibrations. However, those of the Zn^{2+}-IIPs (Fig. 1(d) and (e)) were weakened, maybe because the methyl was lost by A-187 connecting on the attapulgites to form Si–O–Si. It also led the Si–O bands of both Zn^{2+}-IIPs around 1,040 cm^{-1} (Fig. 1(d) and (e)) were a little stronger than that of attapulgite (Fig. 1(a)), and redshifted with reference to that of A-187 (1,070 cm^{-1}, Fig. 1(c)). In addition, the band assigned to naphthenic base at about 915 cm^{-1} was absent in those of Zn^{2+}-IIPs, which inferred that the silylating agent A-187 was bound to Zn–CTS accompanied with ring opening. It would result in a desired Si–O–Si network with a high degree of cross-linking. Therefore, a condensation between the silanol groups from hydrolysis of the siloxane rings and attapulgite surface took place simultaneously.

The surface morphology of attapulgites with and without Zn^{2+}-IIPs was revealed by SEM images (Fig. 2). Attapulgites without Zn^{2+}-IIPs had acicular surfaces with diameters of approximately 0.1 μm and lengths of about 2 μm (Fig. 2(a)). However, after modification to produce Zn^{2+}-IIP, as shown in Fig. 2(b), the surface of attapulgites was covered with cross-linked polymer and became smoother and flatter. With TG (thermogravimetric) analysis (Fig. 3), the attapulgites weight gain between with and without Zn^{2+}-IIPs could be quantified in percentage. TG curve of the attapulgites without Zn^{2+}-IIPs showed three thermal mass loss stages between 20 and 800℃. Stage (1) from about 20 to 180℃ was attributed to the loss of absorbed water or interlayer water, which is the water absorbed between the particles of attapulgite; stage (2) from about 180 to 450℃ was attributed to the loss of water of hydration, which is the water present in the hydrated compounds; and stage (3) from about 450 to 710℃ was attributed to the loss of water of constitution, which is the water held by a unit of structure as

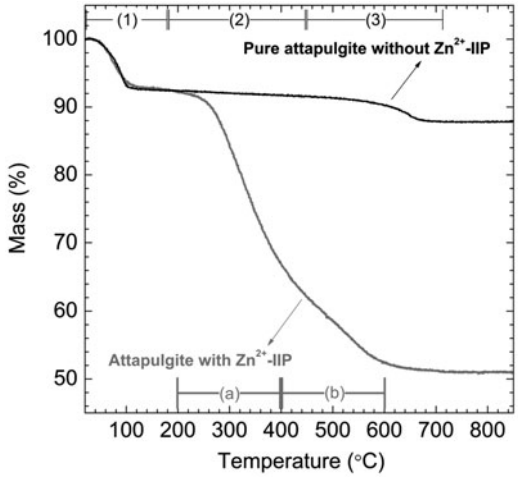

Fig. 3. TG curves of pure attapulgites without Zn^{2+}-IIP and attapulgites with Zn^{2+}-IIP.

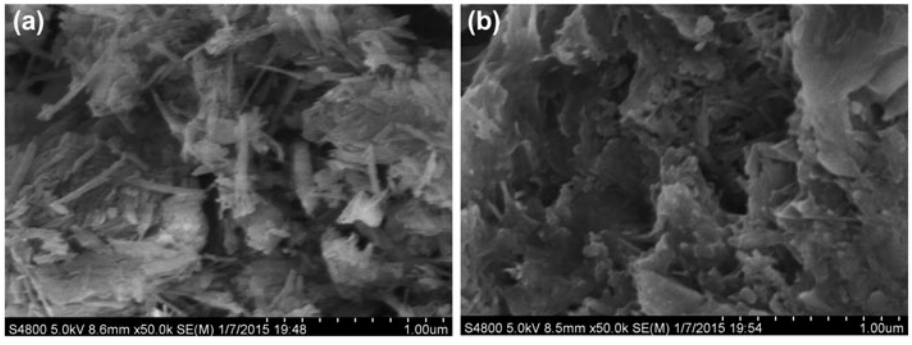

Fig. 2. SEM images: (a) pure attapulgites without Zn^{2+}-IIP and (b) attapulgites with Zn^{2+}-IIP.

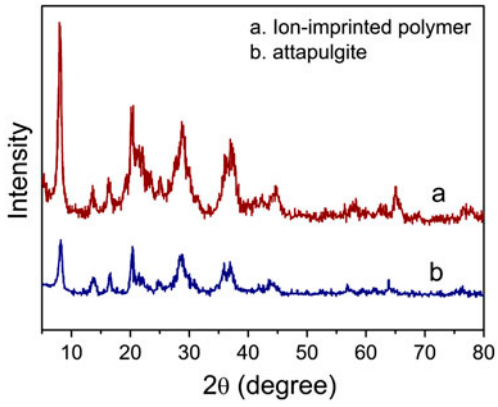

Fig. 4. XRD patterns of raw attapulgite and ion-imprinted polymer.

an essential part of its constitution. In contrast, after modification to form Zn^{2+}-IIP, two extra thermal mass loss stages (marked as (a) and (b) in Fig. 3) emerged: due to organic decomposition (stage (a): about 200 to 400 °C) and due to the loss of –OH and –NH coordinated with Zn^{2+} (stage (b): about 400 to 600 °C). XRD patterns (Fig. 4) showed the ion-imprinted polymer (a) had almost the same crystalline feature with the raw attapulgite (b). A slight shift could be found in Fig. 4(a) compared with the pattern of raw attapulgite, indicating the hybridization between CTS, A-187, and attapulgite. From the obtained peak width of XRD pattern, the particle sizes of ion-imprinted polymer and raw attapulgite can be calculated by the Sherrer formula:

$$D_{hkl} = \frac{K\lambda}{\beta \cos \theta} \quad (6)$$

where $D_{h\ k\ l}$ is the crystal size at the vertical direction of ($h\ k\ l$), λ is the wavelength of X-ray, θ is the angle of diffraction, β is the full-width half-maximum of the diffraction peak, and the constant $K = 0.90$. Accordingly, the mean particle sizes of the attapulgite and ion-imprinted polymer are evaluated as about 12.4 ± 0.2 and 12.1 ± 0.4, respectively. Therefore, the modification of attapulgite neither changed the crystalline structure nor affected the particle size significantly.

3.2. Optimum pH value

The initial pH value of solution is an important parameter affecting the adsorption process, because it affects the protonation of amino group on the IIP. Under acidic conditions, H^+ ions were so active that Zn^{2+} ions cannot successfully occupy the adsorption sites on the IIP. However, with the increase in pH value, the competition from H^+ decreases and Zn^{2+} ions can be adsorbed on the IIP. In the present study, adsorption ratio of adsorbent increased remarkably with increasing pH values up to 7.0. The fraction of Zn^{2+} adsorbed for low C_0 (0.3 meq/L) increased from 0 to unity as pH increased from 3 to 6 (Fig. 5). Only about 75% of the Zn^{2+} in the high C_0 (1.2 meq/L) system was ever adsorbed; this occurred above pH 11. This behavior illustrates the site-specific nature of metal ions adsorption processes. At low Zn^{2+} concentration, the number of available sorption sites on the IIP preferred by Zn^{2+} for geometrical, electrical, or chemical reasons are in excess relative to the number of dissolved Zn^{2+} ions. Only at high Zn^{2+} concentrations, the number of such sites is insufficient to adsorb all available ions in solution and the pH edges become less steep. Precipitation occurred due to the formation of insoluble hydroxide forms of metal when the pH value was higher than 8.0. Accordingly, the pH value of 6.0 was chosen as the optimum condition for further experiments.

The PZC of the samples was influenced by the sites of the attapulgite surface and the functional groups of the polymer coating. The samples underwent hydroxylation in the presence of adsorbed water molecules, forming two types of co-existing hydroxyl groups: the basic-type and the acidic-type. Basic sites accept protons whereas acidic sites donate protons, yielding positively and negatively charged sites, respectively. Thus, lower PZC were found for those containing acid groups, such as Si–OH, and higher values were found for the ones containing basics groups, such as $-NH_2$. After the leaching of Zn^{2+} from IIP, the imprinted cavities were formed, and the cavities accepted protons. As showed in Table 1, the PZC of IIP was lower than that of NIP.

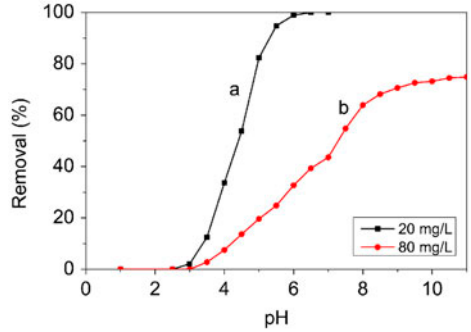

Fig. 5. The influence of pH on the adsorption process at different initial concentration of Zn^{2+} (C_0): (a) C_0 = 0.3 meq/L and (b) C_0 = 1.2 meq/L.

Table 1
The PZC values of the investigated IIP and NIP

	IIP	NIP
PZC	2.6	3.8

3.3. Adsorption kinetics

Before studying the adsorption kinetics, the residual Zn^{2+} content of the IIP after leaching was determined to be 0.0026 meq/g. Fig. 6(a) showed the time dependence curves of the adsorption amount of Zn^{2+} on IIP at different temperature (288, 298, 308, and 318 K). The equilibrium adsorption amount increased with temperature, indicating endothermic processes. The experimental data were analyzed with two models, pseudo-first-order kinetic and pseudo-second-order kinetic. The pseudo-first-order kinetic equation is expressed as:

$$\ln(Q_{e,1} - Q_t) = \ln Q_{e,1} - k_1 t \tag{7}$$

where k_1 is the equilibrium rate constant (1/min), $Q_{e,1}$ and Q_t are the amounts of Zn^{2+} adsorbed at equilibrium and at time t (meq/g), respectively. The pseudo-second-order equation is expressed as:

$$\frac{t}{Q_t} = \frac{1}{k_2 Q_{e,2}^2} + \frac{t}{Q_{e,2}} \tag{8}$$

where k_2 is the equilibrium rate constant (g/meq min) and $Q_{e,2}$ is the equilibrium adsorption amount (meq/g). According to the fitted results in Table 2, the correlation coefficients for the pseudo-first-order kinetic model were very low, indicating a poor pseudo-first-order fit to the experimental data. With an instead, the highly ideal linear relationship between t/Q_t and t on Fig. 6(b) indicated the high correlation coefficients by the pseudo-second-order fitting according to Eq. (8). Hence, the pseudo-second-order kinetic model provided a good correlation for the adsorption of Zn^{2+} onto ion-imprinted polymer in contrast to the pseudo-first-order model.

The activation energy can be considered as the minimum kinetic energy required for a given reaction to take place. Fig. 6(c) shows the temperature dependence of Zn^{2+} sorption by the adsorbent, from which the activation energy could be calculated according to Arrhenius equation:

$$\ln k_2 = -\frac{E_a}{RT} + \ln A_0 \tag{9}$$

where k_2 is the pseudo-second-order equation rate constant (g/meq min), R is the perfect gas constant (8.314 J/mol K), and A_0 is the apparent frequency factor. Thus, the E_a value of Zn^{2+} adsorption on IIP was evaluated as 23.8 kJ/mol. It was lower than that of the typical chemisorption barrier (usually >40 kJ/mol) [24]. So, the sorption mechanism should be a physical sorption, which was driven by van der Waals interaction and weak electrostatic forces, and was accompanied with ion exchange reactions. In the previous relevant studies, cross-linked metal-imprinted chitosan

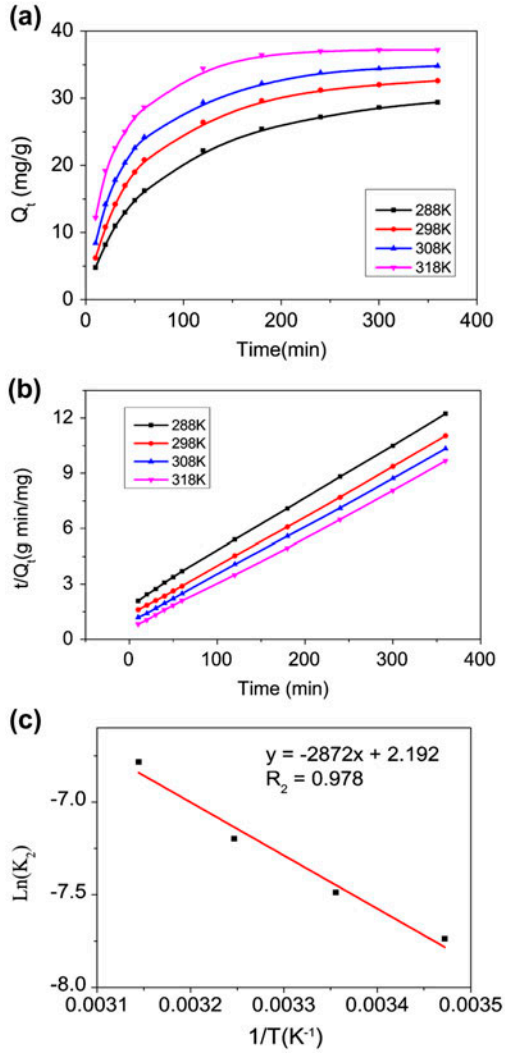

Fig. 6. (a) The adsorption kinetic curves of the adsorption amount of Zn^{2+} on the ion-imprinted polymer (IIP) at different temperatures, (b) the pseudo-second-order fitting of the adsorption kinetic curves at different temperatures, and (c) plot of $\ln(k_2)$ vs. $1/T$ (the points correspond to 288, 298, 308, and 318 K).

Table 2
Kinetic parameters for the adsorption of the Zn^{2+} onto ion-imprinted polymer at different initial concentrations

	Pseudo-first-order			Pseudo-second-order		
T (K)	k_1 (1/min)	$Q_{e,1}$ (meq/g)	R^2	k_2 (g/meq min)	$Q_{e,2}$ (meq/g)	R^2
288	4.92×10^{-3}	0.407	0.9659	2.842×10^{-2}	0.534	0.9998
298	5.45×10^{-3}	0.391	0.9413	3.623×10^{-2}	0.572	0.9998
308	6.04×10^{-3}	0.356	0.9350	4.865×10^{-2}	0.590	0.9999
318	6.72×10^{-3}	0.293	0.8749	7.377×10^{-2}	0.614	0.9996

microparticle was prepared and its adsorption ability for Zn^{2+} was 0.32 meq/g (Q_e, 298 K) [25]. In comparison, the adsorption ability for Zn^{2+} was 0.57 meq/g (Q_e, 298 K) in the present study, showing improved adsorption ability. This is because the cross-linked polymer network was formed on the surface of the attapulgite, with surface cavities more accessible to Zn^{2+} ions during adsorption.

3.4. Adsorption isotherm and the influence of adsorbent concentration (C_a)

Fig. 7(a) shows the adsorption isotherm of Zn^{2+} on ion-imprinted polymer and non-imprinted polymer at different temperatures. The amount of adsorption increased sharply with temperature over low concentrations, but at concentrations higher than 0.3 meq/L, it reached a plateau as the adsorption approached saturation. At 298 K, the maximum static adsorption capacities of IIP and NIP were 0.665 and 0.446 meq/g, respectively. The high adsorption (0.446 meq/g) of NIP was due to the –NH and –OH groups on NIP, but NIP did not selectively adsorb Zn^{2+}. In comparison, IIP had adequate imprinted cavities with high affinity to Zn^{2+}, so display higher adsorption selectivity to Zn^{2+}.

The adsorption data could be fitted by the linear form of Freundlich adsorption model:

$$\ln Q_e = \ln K_F + \frac{1}{n} \ln C_e \tag{10}$$

where Q_e is the equilibrium concentration of Zn^{2+} on adsorbent (meq/g), C_e is the equilibrium concentration of Zn^{2+} in solution (meq/L), and K_F and n are the Freundlich constants (meq/g) related to adsorption capacity and adsorption intensity, respectively. However, the result of the linear fitting had low coefficients of determination ($R^2 < 0.95$, see the left of Table 3). So another model, Langmuir model, was chosen to study the adsorption isotherm at different temperatures. The linear form of Langmuir models is:

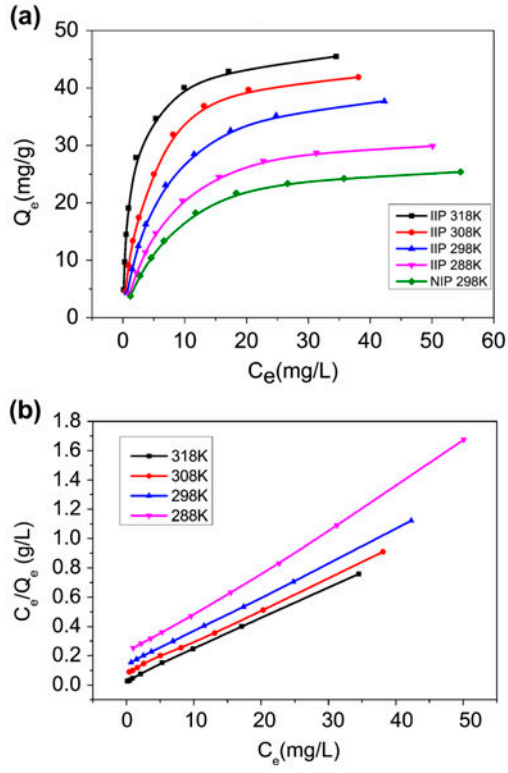

Fig. 7. (a) Adsorption isotherm of Zn^{2+} on ion-imprinted polymer and non-imprinted polymer at different temperatures and (b) the dependence curve of C_e/Q_e on C_e of Zn^{2+} on ion-imprinted polymer at different temperatures. It yields the linear Langmuir adsorption model with high coefficients of determination ($R^2 > 0.99$, see the right of Table 3).

$$\frac{C_e}{Q_e} = \frac{1}{Q_{max} \times K_L} + \frac{C_e}{Q_{max}} \tag{11}$$

where Q_{max} is the maximum amount of Zn^{2+} adsorption (meq/g) and K_L is the Langmuir adsorption constant (L/meq). According to the linear fit between C_e/Q_e and C_e (Fig. 7(b)), the Langmuir model was found to be

Table 3
Adsorption isotherm parameters for the adsorption of the Zn^{2+} onto ion-imprinted polymer at different temperatures

Freundlich model				Langmuir model			
T (K)	n	K_F (meq/g)	R^2	Q_{max} (meq/g)	K_L (L/meq)	R^2	R_L
288	1.933	0.686	0.930	0.536	9.00	0.9982	0.591
298	1.931	0.946	0.946	0.665	10.93	0.9998	0.543
308	2.050	1.138	0.942	0.715	16.97	0.9993	0.433
318	2.657	1.193	0.908	0.722	47.74	0.9993	0.214

more suitable than the Freundlich model, and had higher coefficients of determination ($R^2 > 0.99$, see the right of Table 3). The maximum amounts of Zn^{2+} adsorption were calculated as 0.536, 0.665, 0.715, and 0.722 meq/g at 288, 298, 308, and 318 K, respectively. A constant called equilibrium parameter (R_L) was also used to characterize the Langmuir isotherm:

$$R_L = \frac{1}{1 + C_0 \times K_L} \tag{12}$$

where C_0 is the initial concentration of Zn^{2+} in solution (meq/L). Thus, the effectiveness of an adsorption process can be quantified by R_L: unfavorable ($R_L > 1$), linear ($R_L = 1$), favorable ($R_L < 1$), and irreversible ($R_L = 0$) [26]. The value of R_L was in the range of 0.214–0.591 (Table 3), indicating that the prepared ion-imprinted polymer was a favorable adsorbent to Zn^{2+}.

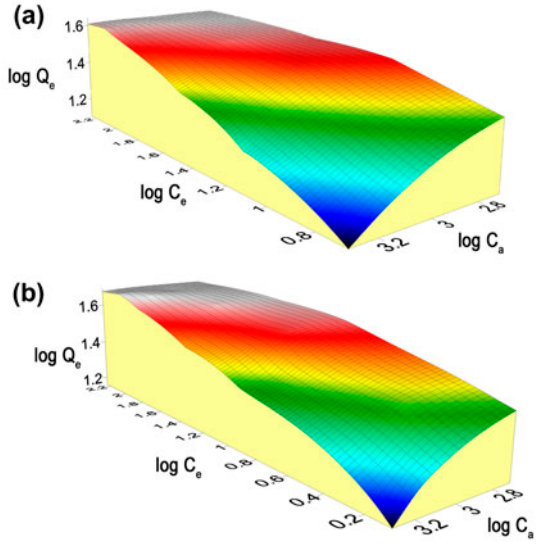

Fig. 8. Influence of adsorbent concentration (C_a) on Zn^{2+} adsorption isotherm at temperatures: (a) 298 and (b) 318 K.

The isotherms for Zn^{2+} sorption on ion-imprinted polymer in these systems was also strongly influenced by adsorbent concentration (C_a). In Fig. 8, the quantity of Zn^{2+} adsorbed by per unit mass IIP (log Q_e) was plotted as functions of both the equilibrium Zn^{2+} concentration (log C_e) and the IIP concentration (log C_a) at 298 K (Fig. 8(a)) and 318 K (Fig. 8(b)), respectively. The plotted surfaces were generated by Kriging model for interpolation between experimental data points. The slope of isotherms increased with increasing C_a; i.e. at higher C_a and lower C_e, unit sorption of Zn^{2+} by IIP decreased. For higher concentrations of Zn^{2+}, any apparent C_a effect was less pronounced. Note that the results presented indicated a strong C_a effect over the lower range of Zn^{2+} concentrations examined, but apparent C_a effect was expected to diminish at higher Zn^{2+} concentrations. Such diminishing trend at 318 K (Fig. 8(b)) was obviously faster than that at 298 K (Fig. 8(a)).

The phenomena may be interpreted in terms of the site-specific nature of the sorption of metals. Here, Zn^{2+} ions are coordinated with the reactive groups (O–H or N–H) of imprinted cavities on the IIP surface. For high IIP concentrations (C_a), an excess of imprinted cavities are available to Zn^{2+} ions, resulting in the dramatic increase in Q_e with increasing C_e. Conversly, at lower IIP concentrations (C_a), Q_e is less influenced by C_e because no extra imprinted cavities are available to Zn^{2+} ions. With an inverse trend, at a high level of the equilibrium Zn^{2+} concentration (C_e) level with increasing C_a, only a very small amount of Zn^{2+} should be excessively added to keep the high level of C_e, as extra active imprinted cavities hardly exist at high C_e and the newly formed active imprinted cavities would be occupied immediately with a cost of slightly decreasing in the quantity of Zn^{2+}. Inversely, at a low level of the equilibrium Zn^{2+} concentration (C_e) level with increasing C_a, a relatively large amount of Zn^{2+} should be excessively added to keep the level of C_e, since there are much more extra active imprinted cavities on IIPs and much more

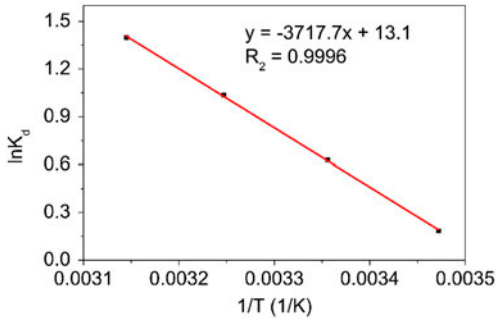

Fig. 9. Plots of ln K_D vs. $1/T$ for the Zn^{2+} adsorption on ion-imprinted polymer.

active imprinted cavities should be occupied to keep the system equilibrium. It requires a great amount of Zn^{2+} to result in a dramatic increase of Q_e.

3.5. Thermodynamic study

The feasibility of the adsorption process was determined by the thermodynamic parameters including Gibbs free energy change (ΔG°), enthalpy (ΔH°), and entropy (ΔS°). Firstly, the equilibrium adsorption constant at various temperatures, K_D, was calculated with Eq. (13):

$$K_D = \frac{Q_e}{C_e} \tag{13}$$

Then, based on van't Hoff plot (Fig. 9), the thermodynamic parameters of ΔH° and ΔS° were obtained as the slope and intercept of the linear variation of ln K_D vs. $1/T$, respectively, according to Eq. (14):

$$\ln K_D = \frac{\Delta S^\circ}{R} - \frac{\Delta H^\circ}{RT} \tag{14}$$

where R is the ideal gas constant (8.314 J/mol K) and T is the absolute temperature (K). Finally, the free energy change ΔG° (kJ/mol) of adsorption can be calculated by Eq. (15):

$$\Delta G^\circ = \Delta H^\circ - T\Delta S^\circ \tag{15}$$

Table 4 summarizes the values of ΔG°, ΔH°, and ΔS° for the adsorption of Zn^{2+} on adsorbent at different temperatures. The adsorption standard enthalpy change (ΔH°) was positive for all cases, indicating that the adsorption is an endothermic process. The positive value of ΔS° suggested the increased randomness at the solid/liquid interface during the adsorption of Zn^{2+} on adsorbent. The negative values of ΔG° in the temperature range of 288–318 K indicated that the adsorption process was feasible and spontaneous. Furthermore, the decrease in the value of ΔG° with rising temperature indicated that the adsorption was more favorable at higher temperatures. This was also

Table 4
Thermodynamic parameters calculated from the sorption data of Zn^{2+} on ion-imprinted polymer

		ΔG° (kJ/mol)			
ΔH° (kJ/mol)	ΔS° (J/mol K)	288 K	298 K	308 K	318 K
30.862	108.664	−0.433	−1.520	−2.607	−3.693

Table 5
Adsorption selectivity of Zn^{2+} ion-imprinted polymer and non-ion-imprinted polymer

		Zn^{2+} ion-imprinted polymer			Non ion-imprinted polymer			
Ions	C_0 (meq/L)	C_e (meq/L)	K_d	K	C_e (meq/L)	K_d	K	K'
Zn^{2+}	0.31	0.024	11.74		0.148	1.07		
Cd^{2+}	0.18	0.086	1.08	10.87	0.085	1.09	0.98	11.07
Cs^{+}	0.15	0.070	1.16	10.12	0.077	0.95	1.13	8.99
Co^{2+}	0.34	0.214	0.58	20.24	0.190	0.78	1.37	14.76
Ba^{2+}	0.15	0.076	0.92	12.76	0.092	0.59	1.81	7.04
Sr^{2+}	0.23	0.153	0.48	24.46	0.117	0.94	1.14	21.49
Pb^{2+}	0.10	0.035	1.74	6.75	0.045	1.13	0.95	7.13

confirmed by the positive ΔH° value, indicating higher temperature was in favor of the adsorption process.

3.6. Selectivity of the Zn^{2+} ion-imprinted polymer

The selectivity of both the Zn^{2+} ion-imprinted polymer and the non-imprinted polymer were investigated by competitive adsorption of Cd^{2+}, Cs^{+}, Co^{2+}, Ba^{2+}, Sr^{2+}, and Pb^{2+} from a mixture. A total of 0.5 g Zn^{2+} ion-imprinted polymer or non-ion-imprinted polymer was equilibrated at pH of 6.0 and 25°C for 5 h with 500 mL of a mixture solution comprising 0.31 meq/L Zn^{2+}, 0.18 meq/L Cd^{2+}, 0.15 meq/L Cs^{+}, 0.34 meq/L Co^{2+}, 0.15 meq/L Ba^{2+}, 0.23 meq/L Sr^{2+}, and 0.10 meq/L Pb^{2+}. The selectivity coefficients (K), distribution coefficients (K_d), and relative selectivity coefficients (K') are given in Table 5.

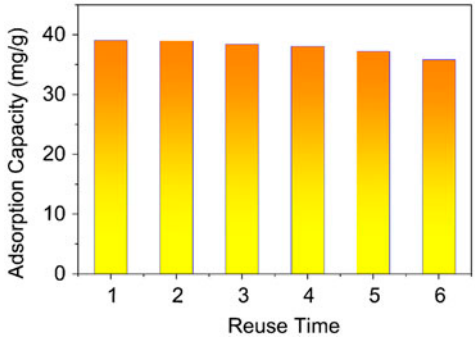

Fig. 10. Reusability of Zn^{2+} ion-imprinted polymer (adsorption: 0.05 g of the Zn^{2+} ion-imprinted polymer uptake 50 mL of 0.77 meq/L Zn^{2+} for 5 h, desorption: 50 mL of 1.0 mol/L HNO_3 at 50°C water bath for 12 h).

The ion-imprinting effect was clearly observed as the Zn^{2+} ion-imprinted polymer had a higher adsorption efficiency of Zn^{2+} than of any other metal ions. This indicated that the Zn^{2+} ion-imprinted polymer had the capability of recognizing Zn^{2+} with higher affinity and selectivity. Moreover, the relative selectivity coefficients (K') being higher than 7 indicated that Zn^{2+} ions can be adsorbed more selectively than other ions, such as Cd^{2+}, Cs^{+}, Co^{2+}, Ba^{2+}, Sr^{2+}, and Pb^{2+}.

3.7. Desorption and reusability

Following the adsorption of the Zn^{2+} ions, the desorption behavior was studied by eluting the Zn^{2+} ions with 50 mL of 1.0 mol/L HNO_3 in water bath at 50°C for 12.0 h. The desorption ratio was determined to be as high as 97.8%, according to Eq. (5). After 6 cycles of adsorption–desorption, the remaining adsorption capacity was still as high as approximately 82.3% of the maximum value (see Fig. 10). This demonstrated that the ion-imprinted polymer can be reused many times without significant degradation in its adsorption capacity.

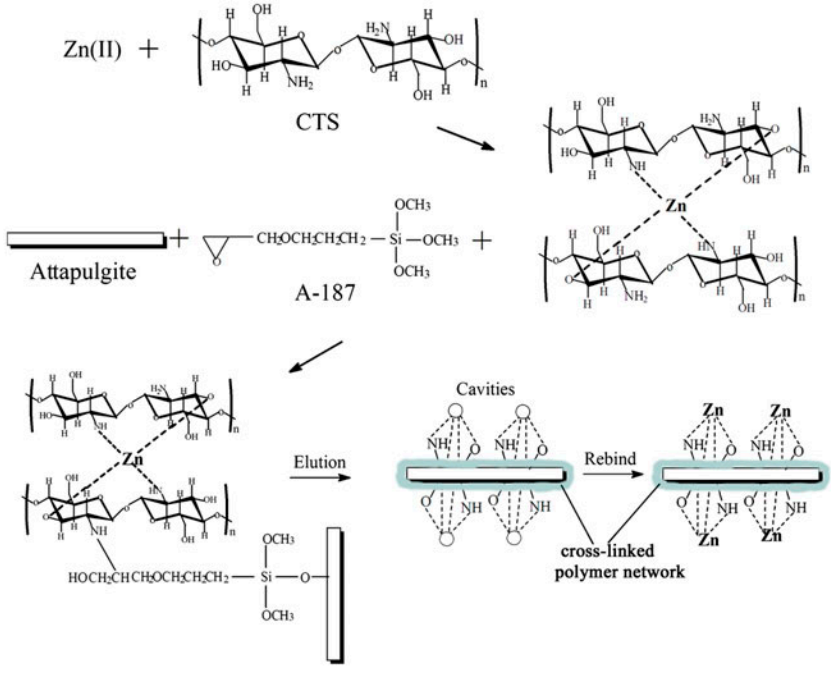

Fig. 11. Imprinting mechanism of the Zn^{2+} ion-imprinted polymer.

3.8. The imprinting mechanism

As shown in Fig. 11, the imprinting mechanism of the Zn^{2+} ion-imprinted polymer can be described as the following process in light of the literatures [27,28]. Firstly, by breaking O–H or N–H, the template Zn^{2+} was coordinated to the functional groups of CTS to form a complex of the CTS–Zn^{2+}. Secondly, addition of attapulgite and A-187 to the complex triggered the following reactions: silanol groups of A-187 were grafted onto the surface of attapulgite through the acid-catalyzed self-hydrolysis, and the epoxy groups of A-187 were broken to connect with the Zn^{2+}-coordinated CTS. Thirdly, the products polymerized to form a cross-linked polymer network on the surface of the attapulgite. Finally, Zn^{2+} ions were leached out from the organic–inorganic hybrid polymer to form imprinted cavities, resulting in a selective key-lock relationship between the cavities and the template Zn^{2+}. Consequently, the ion-imprinted polymer had the capability of recognizing and adsorbing Zn^{2+} with high affinity and selectivity.

4. Conclusions

A new type of Zn^{2+} ion-imprinted polymer (Zn^{2+}-IIP) was synthesized on the surface of attapulgite, displaying high affinity and selectivity for Zn^{2+}. The adsorption isotherm study showed that the Zn^{2+}-IIP was a favorable adsorbent for Zn^{2+} ($0.214 < R_L < 0.591$). The dynamical study showed that the adsorption of the Zn^{2+}-IIP closely followed the pseudo-second-order kinetics equation, with the activation energy, $E_a = 23.8$ kJ/mol, the decreasing negative ΔG° values with rising temperatures, and the positive ΔH° and ΔS° values. It revealed that the adsorption was thermodynamically spontaneous favored at high temperature. After 6 adsorption–desorption cycles, the remaining adsorption capacity of Zn^{2+}-IIP was kept as high as approximately 82.3% of the maximum, demonstrating that the Zn^{2+}-IIP can be reused for many times. So the synthesized Zn^{2+}-IIP proved to be a highly promising candidate for wastewater treatment due to its high selectivity to Zn^{2+} ions and multiple-time reusability with high remaining adsorption capacity.

Acknowledgments

The authors gratefully acknowledge the support from the Science and Technology Innovative Research Team of Zhejiang Province (No. 2009 R50010), Fundamental Research Funds for the Central Universities, Program for Changjiang Scholars, and Program for Innovative Research Team in University of Ministry of Education of China (IRT13R54).

References

[1] G. Zengin, Effective removal of zinc from an aqueous solution using Turkish leonardite–clinoptilolite mixture as a sorbent, Environ. Earth Sci. 70 (2013) 3031–3041.
[2] S.M. Shaheen, F.I. Eissa, K.M. Ghanem, H.M. Gamal El-Din, F.S. Al Anany, Heavy metals removal from aqueous solutions and wastewaters by using various byproducts, J. Environ. Manage. 128 (2013) 514–521.
[3] E. Helios-Rybicka, R. Wójcik, Competitive sorption/desorption of Zn, Cd, Pb, Ni, Cu, and Cr by clay-bearing mining wastes, Appl. Clay Sci. 65–66 (2012) 6–13.
[4] K. Bellir, M.B. Lehocine, A.-H. Meniai, Zinc removal from aqueous solutions by adsorption onto bentonite, Desalin. Water Treat. 51 (2013) 5035–5048.
[5] D. Mohan, K.P. Singh, Single- and multi-component adsorption of cadmium and zinc using activated carbon derived from bagasse—An agricultural waste, Water Res. 36 (2002) 2304–2318.
[6] K. Chong, B. Volesky, Description of two-metal biosorption equilibria by Langmuir-type models, Biotechnol. Bioeng. 47 (1995) 451–460.
[7] A. Zouboulis, K. Matis, Removal of metal ions from dilute solutions by sorptive flotation, Crit. Rev. Environ. Sci. Technol. 27(3) (1997) 195–235.
[8] S. Quek, D. Wase, C. Forster, The use of sago waste for the sorption of lead and copper, WATER SA 24 (1998) 251–256.
[9] Z.A. Othman, M.A. Habila, A. Hashem, Removal of zinc(II) from aqueous solutions using modified agricultural wastes: Kinetics and equilibrium studies, Arab. J. Geosci. 6 (2012) 4245–4255.
[10] A. Sdiri, T. Higashi, R. Chaabouni, F. Jamoussi, Competitive removal of heavy metals from aqueous solutions by montmorillonitic and calcareous clays, Water Air Soil Pollut. 223 (2011) 1191–1204.
[11] A.L.P. de Araujo, M.L. Gimenes, M.A.S.D. de Barros, M.G.C. da Silva, A kinetic and equilibrium study of zinc removal by Brazilian bentonite clay, Mater. Res-Ibero-Am J. 16 (2013) 128–136.
[12] M. Tuzen, M. Soylak, Multiwalled carbon nanotubes for speciation of chromium in environmental samples, J. Hazard. Mater. 147 (2007) 219–225.
[13] H. Ebrahimzadeh, E. Moazzen, M.M. Amini, O. Sadeghi, Novel ion imprinted polymer coated multiwalled carbon nanotubes as a high selective sorbent for determination of gold ions in environmental samples, Chem. Eng. J. 215–216 (2013) 315–321.
[14] M. Khajeh, Z.S. Heidari, E. Sanchooli, Synthesis, characterization and removal of lead from water samples using lead-ion imprinted polymer, Chem. Eng. J. 166 (2011) 1158–1163.
[15] M.E.H. Ahamed, X.Y. Mbianda, A.F. Mulaba-Bafubiandi, L. Marjanovic, Ion imprinted polymers for the selective extraction of silver(I) ions in aqueous media: Kinetic modeling and isotherm studies, React. Funct. Polym. 73 (2013) 474–483.
[16] M.H. Arbab-Zavar, M. Chamsaz, G. Zohuri, A. Darroudi, Synthesis and characterization of nano-pore thallium(III) ion-imprinted polymer as a new sorbent

for separation and preconcentration of thallium, J. Hazard. Mater. 185 (2011) 38–43.
[17] G. Fang, J. Tan, X. Yan, An ion-imprinted functionalized silica gel sorbent prepared by a surface imprinting technique combined with a sol−gel process for selective solid-phase extraction of cadmium(II), Anal. Chem. 77 (2005) 1734–1739.
[18] H. Fan, J. Li, Z. Li, T. Sun, An ion-imprinted amino-functionalized silica gel sorbent prepared by hydrothermal assisted surface imprinting technique for selective removal of cadmium(II) from aqueous solution, Appl. Surf. Sci. 258 (2012) 3815–3822.
[19] Y. Zhan, X. Luo, S. Nie, Y. Huang, X. Tu, S. Luo, Selective separation of Cu(II) from aqueous solution with a novel Cu(II) surface magnetic ion-imprinted polymer, Ind. Eng. Chem. Res. 50 (2011) 6355–6361.
[20] M.H. Bradbury, B. Baeyens, Experimental measurements and modeling of sorption competition on montmorillonite, Geochim. Cosmochim. Acta 69 (2005) 4187–4197.
[21] V.E. dos Anjos, J.R. Rohwedder, S. Cadore, G. Abate, M.T. Grassi, Montmorillonite and vermiculite as solid phases for the preconcentration of trace elements in natural waters: Adsorption and desorption studies of As, Ba, Cu, Cd, Co, Cr, Mn, Ni, Pb, Sr, V, and Zn, Appl. Clay Sci. 99 (2014) 289–296.
[22] K. Bunzl, W. Schimmack, Kinetics of the sorption of Cs-137, Sr-85, Co-57, Zn-65, and Cd-109 by the organic horizons of a forest soil, Radiochim. Acta 54 (1991) 97–102.
[23] Y. Yang, Y. Chun, G. Sheng, M. Huang, pH-dependence of pesticide adsorption by wheat-residue-derived black carbon, Langmuir 20 (2004) 6736–6741.
[24] T. Shahwan, D. Akar, A.E. Eroğlu, Physicochemical characterization of the retardation of aqueous Cs^+ ions by natural kaolinite and clinoptilolite minerals, J. Colloid Interface Sci. 285 (2005) 9–17.
[25] C. Chen, C. Yang, A. Chen, Biosorption of Cu(II), Zn(II), Ni(II) and Pb(II) ions by cross-linked metal-imprinted chitosans with epichlorohydrin, J. Environ. Manage 92 (2011) 796–802.
[26] A. Özcan, C. Ömeroğlu, Y. Erdoğan, A.S. Özcan, Modification of bentonite with a cationic surfactant: An adsorption study of textile dye Reactive Blue 19, J. Hazard. Mater. 140 (2007) 173–179.
[27] Y. Liu, Z. Liu, Y. Wang, J. Dai, J. Gao, J. Xie, Y. Yan, A surface ion-imprinted mesoporous sorbent for separation and determination of Pb(II) ion by flame atomic absorption spectrometry, Microchim. Acta 172 (2010) 309–317.
[28] S. Daniel, J.M. Gladis, T.P. Rao, Synthesis of imprinted polymer material with palladium ion nanopores and its analytical application, Anal. Chim. Acta 488 (2003) 173–182.